

Gernot Eichmann

Towards a microscopic understanding of nucleon polarizabilities

Received: date / Accepted: date

Abstract We outline a microscopic framework to calculate nucleon Compton scattering from the level of quarks and gluons within the covariant Faddeev approach. We explain the connection with hadronic expansions of the Compton scattering amplitude and discuss the obstacles in maintaining electromagnetic gauge invariance. Finally we give preliminary results for the nucleon polarizabilities.

Keywords Nucleon · Compton scattering · Faddeev equations · Dyson-Schwinger approach

1 Introduction

There is much ongoing interest in the precision determination of the nucleon's polarizabilities; see [1] for a recent review. The electric polarizability α and magnetic polarizability β tell us how the nucleon responds to an external electromagnetic field, with current PDG values $\alpha = 11.2(4) \times 10^{-4} \text{ fm}^3$ and $\beta = 2.5(4) \times 10^{-4} \text{ fm}^3$ for the proton [2]. The polarizabilities are proportional to the volume and their smallness indicates that the proton is a rigid object due to the strong binding of its constituents. Whereas $\alpha + \beta$ is constrained by a sum rule, the small value for β is commonly believed to be due to a cancellation between the nucleon 'quark core' and the interaction with its pion cloud.

The polarizabilities are encoded in the nucleon Compton scattering (CS) amplitude $N\gamma^* \rightarrow N\gamma^*$ which has many applications also beyond polarizabilities. The integrated CS amplitude is relevant for two-photon corrections to nucleon form factors [3] and perhaps also for the proton radius puzzle [1]. So far, our knowledge of the CS amplitude is restricted to a few kinematic limits including the (generalized) polarizabilities in real and virtual CS [4], the nucleon structure functions in the forward limit, and deeply virtual CS (DVCS) from where generalized parton distributions are extracted [5]. In addition, the crossed process $p\bar{p} \rightarrow \gamma\gamma$ will be measured by PANDA.

While lattice calculations for polarizabilities are underway (see [1] for references), the main theoretical tools to address CS are 'hadronic' descriptions such as chiral perturbation theory, which provides a systematic expansion of the CS amplitude at low energies [6], and dispersion relations with a direct link to experimental data [7; 8]. On the other hand, handbag dominance in DVCS is well established and a key ingredient to factorization theorems. Is it then possible to connect these two facets by a common, underlying approach at the level of quarks and gluons that reproduces all established features, from hadronic poles to the handbag picture? In the following we will briefly outline such an approach and present first calculated results for the proton polarizabilities α and β .

This work is supported by the German Science Foundation DFG under project number DFG TR-16.

G. Eichmann
Institut für Theoretische Physik, Justus-Liebig-Universität Giessen
Heinrich-Buff-Ring 16, 35392 Giessen, Germany
Tel.: +49 641 9933342
Fax: +49 641 9933309
E-mail: gernot.eichmann@theo.physik.uni-giessen.de

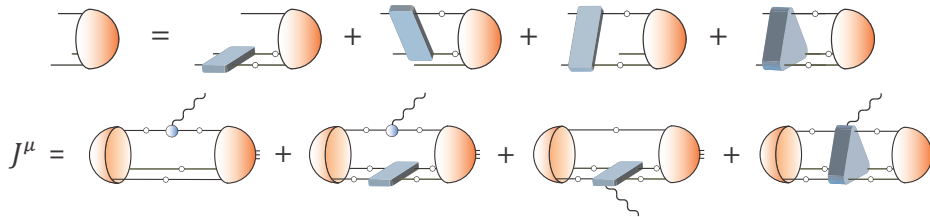


Fig. 1 Three-quark Faddeev equation (top) and electromagnetic current matrix element (bottom).

2 The covariant Faddeev approach

Our tool of choice is the covariant three-body Faddeev approach established in [9]. Its basic equations are illustrated in Fig. 1. The Faddeev equation determines the nucleon mass and bound-state amplitude (its ‘wave function’) by summing up all possible two- and three-body interactions between dressed quarks. The electromagnetic current matrix element couples the photon to all microscopic ingredients and thereby satisfies electromagnetic gauge invariance.

To solve the Faddeev equation one needs to specify its input. Three-body interactions have been neglected so far, and most studies have employed a rainbow-ladder truncation where the two-body kernel is given by a dressed gluon exchange. The dressed quark propagator is solved from its Dyson-Schwinger equation and the resulting quark mass function becomes momentum-dependent; it describes the transition from the input current-quark mass at large momenta to a nonperturbative, dressed ‘constituent quark’ mass of a few hundred MeV in the infrared. In general, any truncation must preserve chiral symmetry to ensure a massless pion in the chiral limit via the analogous Bethe-Salpeter equation; see e.g. [11] for recent advances in this area.

Whereas the applicability of rainbow-ladder in the light-meson sector is mainly limited to pseudoscalar and vector mesons, baryons fare much better: the approach reproduces the octet and decuplet ground state masses within 5–10% [12]. Fig. 2 shows results for the ρ -meson, nucleon and Δ masses as functions of m_π^2 (which is also calculated) compared to lattice data and experiment. The only input is the quark-gluon interaction for the two-body kernel whose model dependence is given by the bands. In particular, once the model scale is set to reproduce the pion decay constant, there are no further parameters or approximations and all subsequent results are predictions.

Apart from mass spectra, a range of form factors have been calculated as well within this setup. Among them are nucleon, Δ and hyperon electromagnetic form factors, the $N \rightarrow \Delta\gamma$ transition, and nucleon axial form factors [13]. All these cases exhibit good overall agreement with experimental data (where available) and also lattice results at larger pion masses, with discrepancies at low Q^2 where pion-cloud effects become important. While the three-body Faddeev approach does not depend on explicit diquark degrees of freedom, it is conceptually close to the quark-diquark framework which typically yields similar results and thereby establishes the presence of strong diquark correlations inside baryons [14]. An advantage is that the approach is not limited to two- and three-body systems: using the very same building blocks, it has been recently also applied to tetraquarks and the muon g-2 problem [15]. Given the body of results so far it is desirable to go a step further and ask: what can we learn about Compton scattering from such a microscopic perspective?

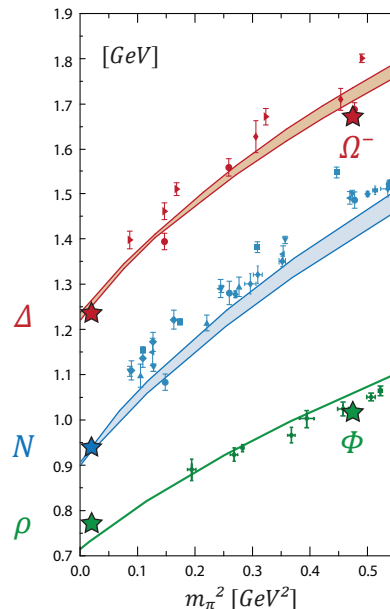


Fig. 2 ρ -meson [10], nucleon and Δ masses [9] calculated from their Bethe-Salpeter and Faddeev equations. Stars are PDG values and symbols with error bars are lattice data (see [9] for references).

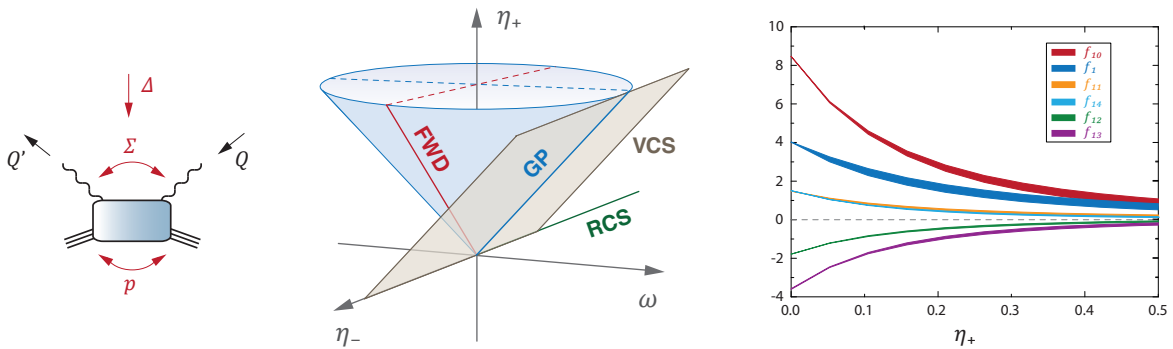


Fig. 3 *Left:* Kinematics and phase space in Compton scattering. *Right:* Dominant Compton form factors corresponding to the residue of the nucleon Born terms after removing the common pole factor. The bands contain the full kinematic dependence on all four variables inside the cone.

3 Compton scattering

The nucleon CS amplitude depends on three independent momenta (see Fig. 3): the average nucleon momentum p , the average photon momentum $\Sigma = (Q+Q')/2$, and the momentum transfer $\Delta = Q-Q'$. The process is described by four Lorentz-invariant kinematic variables which we define as

$$\eta_+ = \frac{Q^2 + Q'^2}{2m^2}, \quad \eta_- = \frac{Q \cdot Q'}{m^2}, \quad \omega = \frac{Q^2 - Q'^2}{2m^2}, \quad \lambda = \frac{p \cdot \Sigma}{m^2}, \quad (1)$$

where m is the nucleon mass. The kinematic phase space in the variables $\{\eta_+, \eta_-, \omega\}$ is illustrated in Fig. 3. The spacelike region that is integrated over in nucleon-lepton scattering forms the interior of a cone around the η_+ axis. Its apex is where the static polarizabilities are defined, with momentum-dependent extensions to real CS ($\eta_+ = \omega = 0$), the doubly-virtual forward limit ($\eta_+ = \eta_-, \omega = 0$), and virtual CS ($\eta_+ = \omega$) including the generalized polarizabilities at $\eta_- = 0$.

Hadronic vs. microscopic decomposition. At the hadronic level the CS amplitude is given by the sum of Born terms, which are determined by the nucleon form factors, and a one-particle-irreducible (1PI) structure part that carries the dynamics and encodes the polarizabilities, see Fig. 4. The latter contains s/u -channel nucleon resonances beyond the nucleon Born terms (including the Δ , Roper, etc.), t -channel meson exchanges (pion, scalar, axialvector, ...), and pion loops, with well-established low-energy expansions in chiral effective field theory. This is usually viewed as the ‘correct’ description at low energies, whereas the handbag picture is interpreted as the ‘correct’ one at large photon virtualities. Hence again the question: is there a common underlying description at the quark level that is valid in *all* kinematic regions and encompasses both approaches?

In analogy to the form factor diagrams in Fig. 1 one can derive a closed expression for the CS amplitude at the quark level [16; 17]. The topologies that survive in a rainbow-ladder truncation (apart from permutations and symmetrizations) are collected in the second row of Fig. 4. Ambiguities stemming from intermediate offshell hadrons never arise here because hadronic degrees of freedom do not appear explicitly. Instead, the diagrams reproduce the onshell hadron pole contributions:

- Diagram (a) depends on the three-quark scattering matrix which contains all possible baryon poles, so it reproduces the nucleon Born terms as well as all s/u -channel resonances.
- Diagram (b) contains the quark two-photon (quark Compton) vertex, which has an analogous decomposition into quark Born terms and a 1PI part. The Born terms provide the handbag contributions. The 1PI part features a quark-antiquark scattering matrix that contains all possible t -channel meson poles and thereby reproduces the meson exchanges in the first row.

Neither the handbag nor the cat’s-ears contributions from diagram (c) have a direct analogue in the hadronic expansion where they are rather absorbed into counterterms. Vice versa, the diagrams in the bottom do not contain the microscopic representation of pion loops because those only enter beyond rainbow-ladder. In any case, the sum of all graphs in the box satisfies electromagnetic gauge invariance

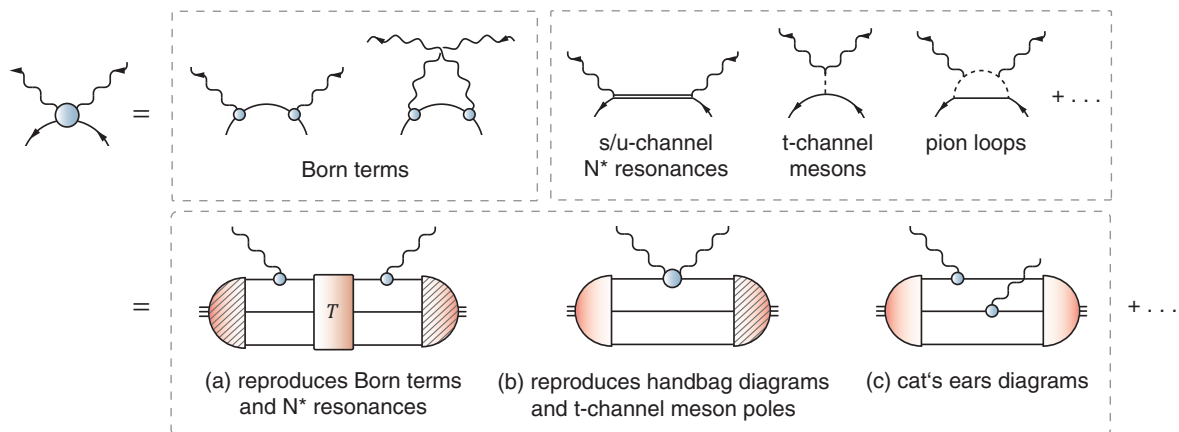


Fig. 4 Hadronic vs. quark-level decomposition of the nucleon Compton scattering amplitude. The first row depicts the hadronic contributions as the sum of Born terms and a 1PI structure part. The latter encodes the polarizabilities and contains s/u -channel nucleon resonances, t -channel meson exchanges and pion loops. The second row shows the microscopic decomposition (in rainbow-ladder) featuring Faddeev amplitudes, quark propagators, quark-photon and quark Compton vertices, and the three-quark scattering matrix [17].

so that the resulting CS amplitude is purely transverse; it is s/u -channel crossing symmetric; it reproduces all known hadronic poles; and it contains the handbag contributions which are perturbatively (and presumably also nonperturbatively) important.

Is it feasible to calculate all these microscopic diagrams in analogy to what has been achieved for form factors? The main obstacle is diagram (a): while there has been progress in the calculation of three- and four-point functions [18], the treatment of six-point functions is so far beyond reach. We therefore approximate this graph by summing up the leading hadronic diagrams in the form of nucleon resonances. Neglecting also diagram (c), we calculate graph (b) in rainbow-ladder but without further approximations: the quark propagator is obtained from its Dyson-Schwinger equation, the nucleon amplitude from the covariant Faddeev equation, and the quark Compton vertex including all (128) tensor structures from its inhomogeneous Bethe-Salpeter equation [17].

Gauge invariance. The problem with this strategy is that only the sum of diagrams (a-c) is gauge invariant but not the individual graphs alone. Since transversality is connected with analyticity, a simple transverse projection does not suffice because an approximation that breaks electromagnetic gauge invariance can induce kinematic singularities that render its results meaningless. The problem can be illustrated with a textbook example, namely the photon vacuum polarization whose general form is $\Pi^{\mu\nu}(Q) = a \delta^{\mu\nu} + b Q^\mu Q^\nu$. The coefficients a and b are functions of Q^2 and must be analytic at $Q^2 = 0$; poles would correspond to intermediate massless particles but since the vacuum polarization is 1PI intermediate propagators are excluded by definition. Gauge invariance entails transversality, $Q^\mu \Pi^{\mu\nu} = 0$, which fixes $a = -b Q^2$. The vacuum polarization can then be written as the sum of a transverse part and a ‘gauge part’ (which is *not* longitudinal):

$$\Pi^{\mu\nu}(Q) = \Pi(Q^2) t_{QQ}^{\mu\nu} + \tilde{\Pi}(Q^2) \delta^{\mu\nu}, \quad t_{AB}^{\mu\nu} = A \cdot B \delta^{\mu\nu} - B^\mu A^\nu. \quad (2)$$

The transverse dressing function $\Pi(Q^2)$ is free of kinematic singularities and zeros. The gauge part $\delta^{\mu\nu}$ is the tensor that we eliminated in the first place, so $\tilde{\Pi}(Q^2)$ must vanish due to gauge invariance. This is what happens in dimensional regularization, whereas a cutoff breaks gauge invariance and induces a quadratic divergence (only) in the gauge part. If we did not know about the decomposition (2) and performed a transverse projection, $\Pi(Q^2)$ would pick up a $1/Q^2$ pole from the gauge part which invalidates the extraction of $\Pi(Q^2 = 0)$. The transverse/gauge separation is also convenient if gauge invariance is broken by more than a cutoff, for instance by an incomplete calculation: ultimately the sum of all gauge parts must vanish, but the partial result for $\Pi(Q^2)$ is still free of kinematic problems and — ideally — not strongly affected by gauge artifacts.

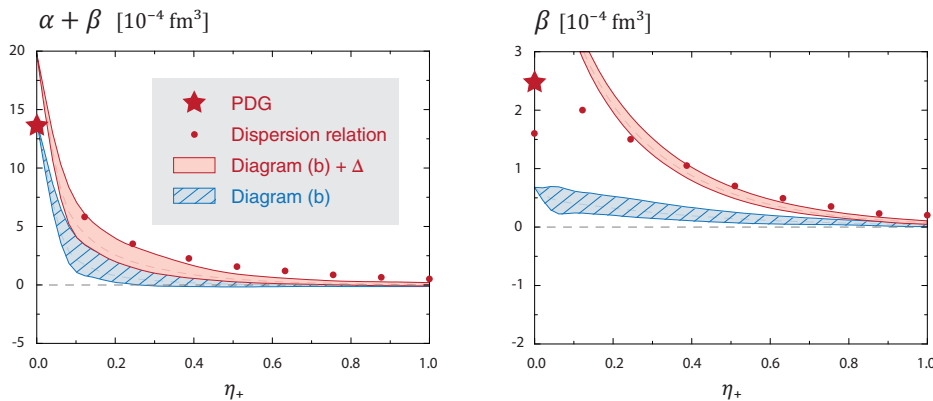


Fig. 5 Proton polarizabilities as functions of η_+ . The bands were obtained from diagram (b) with and without the Δ contribution. The dots were extracted from Ref. [4] and the stars are the experimental values [2].

This simple example also provides the template for the CS amplitude, where a complete decomposition into transverse and gauge parts free of kinematic singularities and zeros is necessary as well:

$$\mathcal{M}^{\mu\nu}(p, Q', Q) = \frac{1}{m} \bar{u}(p_f) \left[\underbrace{\left(\frac{f_1}{m^4} t_{Q'p}^{\mu\alpha} t_{pQ}^{\alpha\nu} + \frac{f_2}{m^2} t_{Q'Q}^{\mu\nu} + \dots \right)}_{\text{transverse part, 18 tensors}} + \underbrace{(\dots)}_{\text{gauge part, 14 tensors}} \right] u(p_i), \quad (3)$$

with $t_{AB}^{\mu\nu}$ defined in Eq. (2). We employ the transverse tensor basis of Refs. [19; 7] but insert factors of ω , λ and m where necessary, so that all Compton form factors (CFFs) $f_i(\eta_+, \eta_-, \omega, \lambda)$ are dimensionless and invariant under photon crossing and charge conjugation. The gauge part must be zero and vanish if all diagrams in Fig. 4 are included. However, even if one breaks gauge invariance by retaining only a subset of diagrams, the transverse CFFs still yield a well-defined prediction.

This can be understood already at the hadronic level. The definition of polarizabilities entails that both the Born and 1PI parts must be individually gauge invariant, so the expansion (3) must hold for both contributions alone. The Born terms are specified by the nucleon's electromagnetic current, but since the intermediate nucleon is offshell the half-offshell nucleon-photon vertex can have more tensor structures. It is well known that only an onshell Dirac current with Q^2 -dependent Pauli and Dirac form factors ensures gauge invariance of the Born term.¹ The right panel in Fig. 3 shows the leading CFFs for this case after removing the common nucleon pole factor. Note that all CFFs are well-behaved and approach constant values for $\eta_+ \rightarrow 0$. As required, the gauge part is exactly zero. The implementation of offshell form factors destroys this property: the gauge part then no longer vanishes but within a reasonable range of model parametrizations the transverse CFFs remain almost unchanged.

Another remarkable feature is visible in Fig. 3: the bands contain the *full* kinematic dependence on all four variables η_+ , η_- , ω and λ inside the cone, but effectively they only depend on η_+ . The residues of the nucleon Born terms therefore scale with η_+ , which reflects the symmetric makeup of the phase space. The hadronic poles form planes in the phase space that will generally counteract this symmetry property: the nucleon Born poles appear at $\eta_- = \lambda = 0$; the nucleon resonance poles form vertical planes at fixed $\eta_- < 0$, where the value of λ depends on the width of the resonance; and t -channel meson poles appear at fixed $\Delta^2 = -m_i^2 \Rightarrow \eta_- = \eta_+ + m_i^2/(2m^2)$.

Polarizabilities. The nucleon polarizabilities α and β are related to the CFFs f_1 and f_2 in the limit where all kinematic variables are zero: $\{\alpha + \beta, \beta\} = \{f_1, f_2\} \times \alpha_{\text{QED}}/m^3$. In Fig. 5 we show preliminary results from the quark-level calculation extracted from the basis in Eq. 3. So far they are only ballpark estimates: the quark Compton vertex that enters in the calculation depends on 6 Lorentz invariants and 128 tensor structures and its transverse/gauge separation is extremely sensitive to the numerics. We extracted the momentum dependence of $\alpha + \beta$ from f_1 only whereas the standard definition [7] contains admixtures from higher CFFs at $\eta_+ > 0$, but for those our results are still too noisy.

¹ For arbitrary offshell form factors the Born terms must be combined with (non-diagrammatic) parts of the 1PI contribution to arrive again at a gauge-invariant expression, see [17] for a discussion.

The hatched bands in Fig. 5 are the outcome of diagram (b) inside the cone. For the total result we added the Δ resonance, the dominant hadronic contribution to diagram (a), using a parametrization for the experimental $N \rightarrow \Delta\gamma$ form factors. For comparison we plot the dispersion relation results for the generalized polarizabilities from Refs. [4; 7]. The figure makes clear that the sum $\alpha + \beta$ is dominated by diagram (b) and, as it turns out, especially by the handbag contributions. The magnetic polarizability β is dominated by the Δ pole from diagram (a) whereas (b) contributes little due to cancellations. The discrepancy at low η_+ is presumably due to missing pion loops — β is subject to cancellations between the quark core (which then mainly comes from the Δ pole) and pion cloud effects.

To summarize, we demonstrated how to extract microscopic information on nucleon polarizabilities from the decomposition in Fig. 4. It will be further interesting to investigate spin polarizabilities and gather knowledge on the spacelike momentum dependence of the CS amplitude, which will improve our understanding of two-photon corrections to form factors as well as the proton radius puzzle. Finally, the same framework can be adapted to other processes such as pion electroproduction, which has contributed much to our knowledge of nucleon resonances and transition form factors. For their clean extraction one needs to know the non-resonant ‘QCD background’ beyond hadronic exchanges, which is information that a microscopic approach can provide.

Acknowledgements I am grateful to C. S. Fischer and G. Ramalho for valuable discussions, and I would like to thank the organizers of the *Light Cone 2015* conference for their support.

References

1. F. Hagelstein, R. Miskimen, and V. Pascalutsa, “Nucleon Polarizabilities: from Compton Scattering to Hydrogen Atom,” [1512.03765\[nucl-th\]](#)
2. K. A. Olive *et al.*, “Review of Particle Physics,” *Chin. Phys.* **C38** (2014) 090001
3. J. Arrington, P. Blunden, and W. Melnitchouk, “Review of two-photon exchange in electron scattering,” *Prog. Part. Nucl. Phys.* **66** (2011) 782–833
4. E. J. Downie and H. Fonvielle, “Real and Virtual Compton Scattering: the nucleon polarisabilities,” *Eur. Phys. J. ST* **198** (2011) 287–306
5. M. Guidal, H. Moutarde, and M. Vanderhaeghen, “Generalized Parton Distributions in the valence region from Deeply Virtual Compton Scattering,” *Rept. Prog. Phys.* **76** (2013) 066202
6. H. W. Griesshammer *et al.*, “Using effective field theory to analyse low-energy Compton scattering data from protons and light nuclei,” *Prog. Part. Nucl. Phys.* **67** (2012) 841–897
7. D. Drechsel, B. Pasquini, and M. Vanderhaeghen, “Dispersion relations in real and virtual Compton scattering,” *Phys. Rept.* **378** (2003) 99–205
8. M. Schumacher and M. D. Scadron, “Dispersion theory of nucleon Compton scattering and polarizabilities,” *Fortsch. Phys.* **61** (2013) 703–741
9. G. Eichmann *et al.*, “Nucleon mass from a covariant three-quark Faddeev equation,” *Phys. Rev. Lett.* **104** (2010) 201601; H. Sanchis-Alepuz *et al.*, “Delta and Omega masses in a three-quark covariant Faddeev approach,” *Phys. Rev.* **D84** (2011) 096003; G. Eichmann, “Nucleon electromagnetic form factors from the covariant Faddeev equation,” *Phys. Rev.* **D84** (2011) 014014
10. P. Maris and P. C. Tandy, “Bethe-Salpeter study of vector meson masses and decay constants,” *Phys. Rev.* **C60** (1999) 055214
11. R. Williams, C. S. Fischer, and W. Heupel, “Light mesons in QCD and unquenching effects from the 3PI effective action,” [1512.00455\[hep-ph\]](#)
12. H. Sanchis-Alepuz and C. S. Fischer, “Octet and decuplet masses: a covariant three-body Faddeev calculation,” *Phys. Rev.* **D90** (2014) no. 9, 096001
13. R. Alkofer *et al.*, “Electromagnetic baryon form factors in the Poincaré-covariant Faddeev approach,” *Hyperfine Interact.* **234** (2015) no. 1-3, 149–154; H. Sanchis-Alepuz and C. S. Fischer, “Hyperon elastic electromagnetic form factors in the space-like momentum region,” [1512.00833\[hep-ph\]](#)
14. G. Eichmann *et al.*, “Toward unifying the description of meson and baryon properties,” *Phys. Rev.* **C79** (2009) 012202; I. C. Cloet *et al.*, “Survey of nucleon electromagnetic form factors,” *Few Body Syst.* **46** (2009) 1–36; J. Segovia, “Elastic and Transition Form Factors in DSEs,” [1601.00973\[nucl-th\]](#).
15. G. Eichmann, C. S. Fischer, and W. Heupel, “The light scalar mesons as tetraquarks,” *Phys. Lett.* **B753** (2016) 282–287; G. Eichmann, C. S. Fischer, W. Heupel, and R. Williams, “The muon $g-2$: Dyson-Schwinger status on hadronic light-by-light scattering,” in *Confinement XI, 2014*. [1411.7876\[hep-ph\]](#).
16. G. Eichmann and C. S. Fischer, “Unified description of hadron-photon and hadron-meson scattering in the Dyson-Schwinger approach,” *Phys. Rev.* **D85** (2012) 034015
17. G. Eichmann and C. S. Fischer, “Nucleon Compton scattering in the Dyson-Schwinger approach,” *Phys. Rev.* **D87** (2013) no. 3, 036006
18. G. Eichmann, C. S. Fischer, and W. Heupel, “Four-point functions and the permutation group S_4 ,” *Phys. Rev.* **D92** (2015) no. 5, 056006
19. R. Tarrach, “Invariant Amplitudes for Virtual Compton Scattering Off Polarized Nucleons Free from Kinematical Singularities, Zeros and Constraints,” *Nuovo Cim.* **A28** (1975) 409